



Fabrication, characterization, and application of pea protein-based edible film enhanced by oregano essential oil (OEO) micro- or nano-emulsion

Jingjing Cheng, Frank J. Velez, Prashant Singh, Leqi Cui*

Department of Health, Nutrition, and Food Sciences, Florida State University, Tallahassee, FL, 32306, USA

ARTICLE INFO

Handling Editor: Dr. Xing Chen

Keywords:

Pea protein
Oregano essential oil
Active film
Nano-emulsion
Antimicrobial activity

ABSTRACT

Pea protein isolate (PPI)-based active films were prepared by incorporating 0.5 %, 1.0 %, or 2.0 % of oregano essential oil (OEO), either in the form of micro-emulsion (MOEO) or nano-emulsion (NOEO). The particle size and polydispersity index of OEO droplets were 2755.00 nm and 0.63 for MOEO, and 256.30 nm and 0.20 for NOEO. The surface and cross-sectional SEM results revealed the presence of holes and internal pores within the film upon the addition of OEO. The molecular interaction between PPI and OEO was confirmed by FTIR. The addition of OEO significantly increased film thickness, decreased water contact angle, and imparted a more yellow color. At a low concentration (0.5 %), the addition of OEO significantly improved the water vapor barrier and mechanical properties of the film. However, at higher concentrations, these film properties were significantly weakened. Additionally, the film antimicrobial properties were assessed after OEO addition. In vitro inhibition zone results indicated that a 2.0 % addition of OEO significantly suppressed the growth of three *Salmonella* strains [*Salmonella* Typhimurium (ATCC14028), *Salmonella* Infantis 94-1, and *Salmonella* Enteritidis PT-30]. Application of pea protein-based film with 2.0 % OEO on chicken breast demonstrated significant reduction in microbial count. Our results further showed that reducing the particle size of OEO from micrometer-scale to nanometer-scale in the PPI film matrix did not significantly alter film properties or antimicrobial activities. The study demonstrated that the antibacterial film based on pea protein and OEO is an innovative food packing material for prohibiting bacteria growth on poultry products.

1. Introduction

Pea protein, as one of the most abundant plant proteins, is widely utilized in the food industry due to its high yield, cost-effectiveness, and availability (Lu et al., 2020). Contrary to soy protein, pea protein is often considered a low-risk allergen and remains free from genetic modification (Lam et al., 2018). Consequently, the applications of pea protein in the food industry have gathered substantial attention. In the field of edible films, pea protein demonstrates its value with good film-forming capability and excellent ultraviolet barrier properties (Ge et al., 2020), and its mechanical and water-resistant properties have recently reported to be improved by techniques such as ultrasound and high-pressure homogenization (Cheng et al., 2022; Cheng and Cui, 2021). These enhancements are further expected to expand the utilization of pea protein-based edible films in the food packaging industry.

Active packaging involves integrating antibacterial and antioxidant agents into food packaging to impart the packaging with properties that combat spoilage associated with bacterial growth and oxidation,

thereby extending the shelf life of the packaged food (Chen et al., 2019). Compared to conventional passive packaging, which primarily offers a physical barrier between the product and its external environment, active films are strategically designed to interact with the packaged product or its surroundings, proactively modifying the packaging environment (Yildirim et al., 2018). Essential oils (EOs), derived from plants, are natural substances recognized for their potent antimicrobial and antioxidant properties (Bhavaniramy et al., 2019). The essential oils can be incorporated into biopolymer film-forming dispersions to produce antimicrobial packaging materials, effectively extending the shelf life of food products (Hashim et al., 2024; Jouki et al., 2014a; Yang et al., 2023).

The primary antibacterial component in OEO is carvacrol, which possesses strong anti-inflammatory and antimicrobial properties, accounting for 65 %–90 % of the total OEO composition (Bonfanti et al., 2012; Hao et al., 2022). Although the antibacterial activity of oregano essential oil (OEO) in edible films has been recognized by previous studies (Otoni et al., 2014b; Zinoviadou et al., 2009), the effective

* Corresponding author.

E-mail address: lcui2@fsu.edu (L. Cui).

antibacterial activity of OEO varies in different film matrices. For example, in alginate film matrix, 1 % of OEO can inhibit the growth of *Salmonella* (Benavides et al., 2012), while in quince seed mucilage film, the concentration of OEO needs to be increased to 1.5 % for the inhibitory effect (Jouki et al., 2014b). However, when incorporating OEO into polylactic acid film, even at an increased concentration of 5 %, there was still no antibacterial effect against *Salmonella* (Llana-Ruiz-Cabello et al., 2016). The discrepancy can be explained by the fact that the EO release rate is related to the interactions between active agent in EO and film components (Teixeira et al., 2014), highlighting that the antibacterial activity of essential oils in edible films is a case-by-case study. Therefore, it is necessary to determine the actual antibacterial activity of OEO after the integration of OEO into pea protein films.

A common method for incorporating essential oils into active films or coatings involves the creation of an emulsion solution, where they are uniformly dispersed within the film-forming mixture (Zhang et al., 2022). To enhance the mixing and retention of essential oils within the film-forming dispersion, researchers have introduced the use of nano-emulsion, which is defined as an emulsion in which the dispersed phase forms droplets at the nanometer scale, typically in the range of 50–500 nm in diameter (Nor Bainun et al., 2015). Research has indicated that nano-emulsions, due to their smaller particle size and larger surface area, can enhance the ability of the active compound to migrate from films and penetrate microbial cells (Otoni et al., 2014a). This property has been reported to contribute to an improved antimicrobial performance of essential oils within packaging films (Cai et al., 2020). Nevertheless, some researchers argue that reducing the particle size of essential oils to the nano-scale does not alter their antimicrobial activity significantly, while the antimicrobial activity remains primarily determined by the effective active compounds present in the essential oils (Buranasuksombat et al., 2011; Liao et al., 2021; Salvia-Trujillo et al., 2015). This apparent paradox is unsurprising, given that the transition from the packaging material to the manifestation of antimicrobial effects on the food surface involves a complex and protracted process. The realization of essential oils' antimicrobial activity depends not only on the properties of the essential oils themselves, but also on the migration of active compounds from package to food, which can be influenced by the interactions between antimicrobial agent and the polymer matrix (Atarés and Chiralt, 2016; Avila-Sosa et al., 2012). This complex interplay plays a crucial role in determining the overall effectiveness of essential oils in active packaging systems, and therefore can be different in various combinations of essential oil-protein matrix.

Based on this background, this study specifically focused on oregano essential oil (OEO) and its incorporation into the pea protein-based film matrix in either micro-emulsion or nano-emulsion format. To the best of our knowledge, no studies have incorporated essential oils into pea protein-based films for enhanced antimicrobial properties. The aim of this study was to investigate the influence of various concentrations and particle sizes of OEO on the structure and properties of pea protein-based films, including color, mechanical properties, water resistance, and antimicrobial activities. Additionally, we evaluated the efficacy of fabricated films in inhibiting the growth of bacteria on chicken breast.

2. Materials and methods

2.1. Materials

Yellow pea protein isolate (PPI) was purchased from Naked Nutrition (Miami, FL, USA). The protein content was 90 %, the fat and carbohydrate content were 2 % and 7 %, respectively. Pure oregano essential oil (OEO) was purchased from Silky Scents, LLC. (Corona, CA, USA). Glycerol (≥ 99 %) was purchased from Sigma (St. Louis, MO, USA). The bacterial strains of *Salmonella* Typhimurium (ATCC 14028), *Salmonella* Infantis 94-1, *Salmonella* Enteritidis PT-30 were obtained from the FSU food microbiology laboratory culture collection (Tallahassee, FL, USA).

2.2. Preparation and characterization of OEO emulsions

The micro-emulsion (MOEO) was prepared by adding PPI (2 %, w/w) to deionized water and stirring for 4 h, followed by addition of OEO (10 %, w/w) and another 1 h of stirring. The solution containing the oil and aqueous phases was then mixed using a high-speed homogenizer (IKA T25 digital ultra-turrax, Staufen, Germany) at 13,000 rpm for 3 min. To obtain nano-emulsion (NOEO), the micro-emulsion was processed with high pressure at the level of 30,000 psi with 3 passes using a high-pressure homogenizer (Nano DeBEE high pressure homogenizer, BEE International, USA). A heat exchanger with a flow of cold water was employed to minimize the temperature increase during homogenization. The emulsions were freshly prepared for the following preparation of film-forming dispersions. The average droplet size (z-average), polydispersity index (PDI) of the emulsions were determined using a Zeta-sizer (Nano ZS90, Malvern Instruments, UK) according to Cui et al. (2019) with some modifications. Before the measurements, the samples were diluted at a 1:125 ratio to minimize the multiple scattering effect. All measurements were conducted at 25 °C.

2.3. Preparation and characterization of PPI-based active films

2.3.1. Film preparation

The method was referenced in a previous study with some modifications (Choi and Han, 2001). The films were prepared by firstly dissolving appropriate amount of PPI (the PPI concentration in the final film-forming dispersion is 7.5 wt%) in deionized water and stirred for 4 h. Subsequently, various amounts of MOEO or NOEO emulsions were added to the film-forming dispersion, resulting in final OEO contents of 0.5 %, 1.0 %, and 2.0 % (w/w) of film-forming dispersions. Then glycerol was added at a 50 % mass ratio to the protein and stirred for 30 min. After degassing, 8 mL of the prepared dispersions were poured onto a Petri dish with a diameter of 10 cm, followed by drying for 24 h at 25 °C. The above samples were labeled as 0.5 % MOEO, 1.0 % MOEO, 2.0 % MOEO, 0.5 % NOEO, 1.0 % NOEO, 2.0 % NOEO, respectively, and PPI film without OEO was prepared as control. We did not study higher OEO concentration because it would completely disrupt the film structure, preventing the formation of an intact film. In the final film-forming dispersion, the total PPI content from both the PPI dispersed in water and the PPI used as an emulsifier in the emulsions was 7.5 wt%. After drying, the films were peeled off and conditioned to 55 % relative humidity at 25 °C for 3 days.

2.3.2. Film thickness

Film thickness was determined using a manual digital micrometer with an accuracy of 0.01 mm. Measurements were taken at 5 randomly selected points. The acquired values were subsequently utilized in the calculations of water vapor permeability (WVP) and mechanical properties.

2.3.3. Scanning electron microscopy (SEM)

The method was based on a previous study with several modifications (Ghamari et al., 2022). Surface and cross-sectional analysis of the films were conducted using a field emission scanning electron microscope (JSM-IT800, JEOL Ltd., Japan) to assess their microstructure and morphology. For this purpose, film samples were fractured manually using liquid nitrogen to create cross-sections. These prepared films were then mounted on a holder and coated with uranium using a Cressington Carbon Coater (Cressington Scientific Instruments Ltd., Watford, UK). The accelerating voltage applied was set at 5.0 kV. The surface and cross-section photographs were taken at 100 × and 1000× magnifications, respectively.

2.3.4. Fourier transform infrared spectroscopy (FTIR)

The infrared spectra of the films were recorded using a FTIR-ATR (JASCO 6800, JASCO, Japan) with a 4 cm⁻¹ resolution in the range of

4000-400 cm⁻¹ (Ghadetaj et al., 2018). Prior to scanning each sample, background data was collected. The final spectra were the result of noise elimination, baseline correction, and smoothing processing.

2.3.5. Moisture content (MC) and total soluble matter (TSM)

The MC and TSM were measured according to the method described by Muñoz et al. (2012). Concisely, the film was first cut into pieces, with each piece carefully weighed, and then was placed in an oven at 105 °C for 24 h. Afterward, the samples were re-weighed, and the MC was calculated based on the percentage of weight loss. To measure TSM, dried film pieces were immersed in 30 mL of deionized water at 25 °C for 24 h. Afterward, undissolved film pieces were filtered using pre-weighed, desiccated filter paper, dried for 24 h at 105 °C, and weighed to determine the weight of insoluble dry matter. TSM was defined as the percentage of soluble dry matter relative to the initial dry matter weight.

2.3.6. Water vapor permeability (WVP)

The water vapor permeability (WVP) was determined in accordance with ASTM Standard Test Method (ASTM, 1995). Each 2 cm × 2 cm film was sealed on top of a glass vial previously filled with silica gel. These vials were then positioned in a chamber preconditioned with deionized water and weighed at 12-h intervals for 2 days. WVP was calculated as:

$$WVT = \frac{\Delta m}{\Delta t \times A}$$

$$WVP = \frac{WVT \times l}{\Delta p}$$

where WVT is water vapor transmission rate (g/h m²); $\Delta m/\Delta t$ is the slope of linear regression equation of weight gains (g) as a function of time (h); A is the area of film exposed to the environment (m²); l is the thickness of films (mm); Δp is the partial vapor pressure difference across the two sides of the film (2.895 kPa).

2.3.7. Water contact angle (WCA)

The WCA values were determined using a sessile drop method, employing a drop shape analyzer (DSA25, Kruss, Germany). A 3 μ L droplet of deionized water was deposited onto the film surface at 25 °C, and its image was captured. Subsequently, the WCA was calculated using KRÜSS ADVANCE software (Kruss, Germany).

2.3.8. Tensile strength (TS) and elongation at break (EAB)

The method used to measure TS and EAB was adopted from a prior study (Cheng et al., 2023). A film strip (20 mm × 60 mm) was vertically secured to the TA. XTplus texture analyzer (Stable Micro System Ltd., Godalming, UK) using two grips initially spaced 20 mm apart. It was then stretched at a force rate of 2 mm/s. TS was determined by dividing the peak load by the cross-sectional area of the film strip (film thickness × 20 mm). EAB was defined as the ratio of the maximum elongation distance (mm) to the initial distance (20 mm).

2.3.9. Color

The color of the films was evaluated using a colorimeter (LabScan XE, HunterLab, Reston, VA, USA) and expressed in terms of L (darkness/whiteness), a (greenness/redness), and b (blueness/yellowness) values. Measurements were collected from five different locations on each film.

2.3.10. In vitro antimicrobial activity

The antimicrobial properties of PPI-based active films were assessed using the agar diffusion method, with a focus on their inhibitory effects against *Salmonella* strains, including *Salmonella* Typhimurium (ATCC14028), *Salmonella* Infantis 94-1, and *Salmonella* Enteritidis PT-30. The antimicrobial properties were evaluated as previously described by Benavides et al. (2012) and Hudzicki (2009). In brief, the microorganisms were cultured by incubating them in tubes containing

10 mL of tryptic-soy broth (TSB, Hardy Diagnostics, Santa Maris, CA, USA) for 24 h at 37 °C. To obtain isolated colonies, the over-night culture was streaked onto a plate count agar (PCA, BD Difco, Franklin Lakes, NJ, USA) plate and incubated at 37 °C for 24 h. Subsequently, a single isolated colony was selected and diluted with 0.85 % saline solution until 0.5 of McFarland turbidity was achieved, resulting in an inoculum containing approximately 1.5×10^8 CFU/mL of bacteria. To measure the inhibition zones, Mueller-Hinton agar (MHA, Hardy Diagnostics, Santa Maria, CA, USA) plates were spread-plated with 100 μ L of the inoculum and then 15 mm film discs were placed on inoculated plates, which were incubated at 37 °C for 24 h. The diameter of the obtained inhibition zones around the discs was measured. These measurements were performed in duplicate for each film.

2.4. Application to chicken breast

2.4.1. Chicken sample preparation

The preparation of the chicken sample followed a previous method with some modifications (Yıldırım-Yalçın et al., 2021). Fresh chicken breast was procured from a local market (Publix, Tallahassee, USA) and cut into 3 × 3 × 1 cm³ samples with each sample weighing approximately 10 g. These samples were then coated with each film-forming dispersion and subsequently wrapped by the respective treated film. Chicken samples without packaging were used as control and the samples packaged using plastic films (cling wrap, PVC) were also prepared for comparison purpose. Specifically, each chicken sample was immersed in 300 mL of the respective film-forming dispersion for 3 min and subsequently allowed to drain for 10 min (the control group and plastic group were treated with cold deionized water to compensate for possible physical removal of bacteria and for moisture uptake). Afterward, the chicken samples were individually wrapped by the corresponding film, placed in a sterile sample bag, and then stored at 4 °C for 10 days. Aerobic plate count was conducted at 2-day intervals during storage.

2.4.2. Aerobic plate count (APC)

The measurement of APC of chicken breast was performed as previously described by Hematizad et al. (2021) with some modifications. Briefly, Chicken breast samples weighing 10 g were transferred under sterile conditions into individual stomacher bag (Nasco, WI, USA). Each bag contained 90 ml of 0.1 % (w/v) sterile peptone water. The samples were then homogenized for 120 s using a stomacher at 260 rpm. For each sample, appropriate serial decimal dilutions were prepared using 0.1 % peptone water. To determine the APC, 100 μ L of the serial dilutions of chicken homogenates were spread onto the surface of PCA. The agar plates were then incubated at 30 °C for 48 h (Gravity Convection Incubator, VWR, USA). After the incubation period, the colonies that grew on the agar plates were counted, and the total mesophilic aerobic bacteria was determined.

2.5. Statistical analyses

All experiments were conducted in triplicate, and the results were reported as mean \pm standard deviation (SD). Statistical significance ($p < 0.05$) was determined using Duncan's multiple comparison test with SPSS version 25.0 (SPSS Inc., Chicago, IL, USA).

3. Results and discussion

3.1. Partial size and PDI of OEO emulsions

It is essential to confirm the successful production of the nano-emulsion before assessing its impact on the properties of the PPI film. In this study, we broke down the OEO droplets into nano-scale in the emulsions by using high-pressure homogenization, which created disruptive forces including turbulence and cavitation. The particle size

distribution, average particle size, and polydispersity index (PDI) obtained for OEO droplets in micro-emulsion (MOEO) and nano-emulsion (NOEO) are shown in Fig. 1. As expected, the particle size of the MOEO was at the micrometer level (Z-average: 2755.00 nm) and following high-pressure treatment its particle size was markedly decreased to the nanometer level (Z-average: 256.30 nm). Additionally, the PDI value for NOEO was 0.20, which is significantly lower than the 0.63 value for MOEO, indicating a narrow particle size distribution range. Similarly, Cai et al. (2020) reported that, with high pressure homogenization treatment at 50 MPa for 5 passes, the Z-average and PDI of ginger essential oil emulsion decreased significantly from 799.53 nm to 0.316–114.71 nm and 0.251, respectively. The reduction in particle size and PDI values of emulsions is a consequence of the intense stress, turbulence, and cavitation induced by high pressure (Donsi and Ferrari, 2016). These results suggested that the OEO droplets were broken down during the high-pressure process, resulting in a more uniform nano-emulsion with smaller particles.

3.2. Characterization of the PPI-based active films

3.2.1. Film thickness

As shown in Table 1, the average thickness of the PPI film was 0.16 ± 0.01 mm. Low concentrations of OEO (0.5 % and 1.0 %) addition did not significantly alter the film thickness. However, at an OEO concentration of 2.0 %, a noticeable increase in film thickness was observed. Furthermore, there were no significant differences ($p > 0.05$) in thickness between MOEO and NOEO films with the same concentrations.

3.2.2. Scanning electron microscopy (SEM)

The scanning electron microscopy (SEM) micrograph provides a direct view of the microstructure of films, which is useful as the film structure is closely related to film properties, including WVP and mechanical properties. To better observe structural changes after adding OEO, SEM analysis was conducted on the films with the maximum OEO addition (2.0 %), as shown in Fig. 2. The surface of the PPI film was homogeneous with a rough texture and without any holes, indicating the integrity of the pure PPI film structure (Fig. 2a). After the addition of 2.0 % MOEO, the film surface displayed numerous holes, which could be due to oil droplets, indicating the successful addition of OEO (Fig. 2b). Similar results were observed in other studies (Zhang et al., 2021; Zhao et al., 2022). Additionally, the holes on the 2.0 % NOEO film were smaller than those on the 2.0 % MOEO film surface, confirming that the

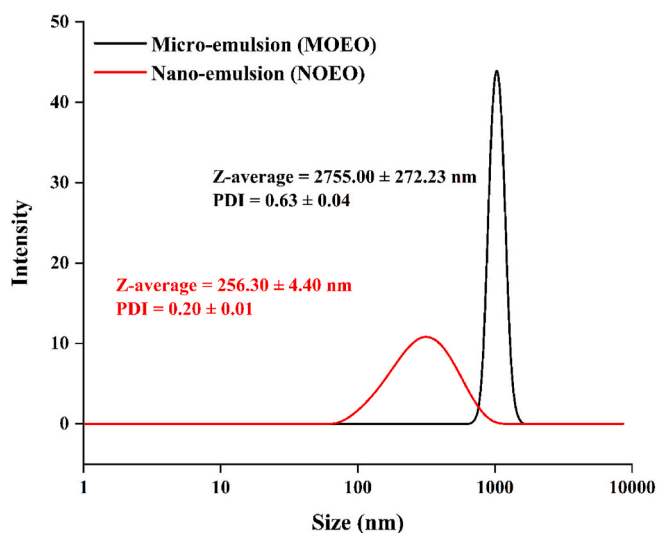


Fig. 1. Particle size distribution, particle size, and polydispersity index (PDI) of oregano essential oil (OEO) micro-emulsion (MOEO) and nano-emulsion (NOEO).

Table 1

The thickness, moisture content (MC), total soluble matter (TSM), water vapor permeability (WVP), and water contact angle (WCA) of pea protein-based active films containing micro- (MOEO) or nano- (NOEO) oregano essential oil.

Film samples	Thickness (mm)	Moisture content (%)	Total soluble matter (%)	WVP (g mm h ⁻¹ m ⁻² kPa ⁻¹)	Water contact angle (°)
PPI	0.16 ± 0.01 ^a	26.50 ± 1.01 ^{ab}	31.19 ± 2.18 ^a	1.65 ± 0.00 ^b	57.94 ± 9.17 ^c
0.5 % MOEO	0.16 ± 0.00 ^{ab}	24.97 ± 2.43 ^{ab}	29.52 ± 4.71 ^a	1.58 ± 0.06 ^{ab}	51.12 ± 2.89 ^b
0.5 % NOEO	0.15 ± 0.01 ^a	27.58 ± 0.95 ^b	33.86 ± 0.65 ^a	1.48 ± 0.06 ^a	51.57 ± 4.49 ^{bc}
1.0 % MOEO	0.17 ± 0.01 ^{bc}	25.35 ± 3.19 ^{ab}	30.22 ± 3.72 ^a	1.75 ± 0.11 ^c	49.26 ± 4.04 ^b
1.0 % NOEO	0.16 ± 0.00 ^{ab}	24.80 ± 2.90 ^{ab}	32.01 ± 5.72 ^a	1.54 ± 0.00 ^{ab}	52.11 ± 7.31 ^{bc}
2.0 % MOEO	0.19 ± 0.02 ^c	21.89 ± 3.37 ^a	30.06 ± 2.53 ^a	1.95 ± 0.00 ^d	42.64 ± 9.09 ^a
2.0 % NOEO	0.18 ± 0.01 ^c	26.80 ± 1.97 ^b	31.67 ± 2.57 ^a	1.77 ± 0.07 ^c	47.35 ± 3.62 ^{ab}

Different letters within the same column are significantly different ($p < 0.05$).

addition of nano-emulsion indeed reduced the size of OEO droplets distributed within the protein matrix (Fig. 2b and c). As for the cross-section, the PPI film exhibited a structure resembling a brick wall, with layers stacked on top of each other (Fig. 2 A). However, when MOEO was added to the film matrix, noticeable pores appeared within the film (see the blue arrows in Fig. 2 B), while some of the pores decreased in size when NOEO was incorporated (the blue arrows in Fig. 2 C). This is consistent with previous findings by Otoni et al. (2014b), who observed smaller oil droplets within the methylcellulose-based film when the size of the essential oil emulsion was reduced. Overall, both the surface holes and cross-sectional pores indicated that OEO was distributed within the film matrix in varying particle sizes.

3.2.3. FTIR

FTIR analysis was carried out to determine the potential interactions between PPI and OEO in the format of either micro-emulsion or nano-emulsion. The spectra of film samples from 4000 cm⁻¹ to 400 cm⁻¹ are shown in Fig. 3. The wavenumbers ranging from 3750 cm⁻¹ to 3000 cm⁻¹ are associated with the stretching vibration of O–H and N–H (Yilmaz et al., 2020). The intensity of the peak in this range increased significantly following the addition of OEO, pointing to a notable rise in the number of free N–H or O–H groups. In this study, this observed enhancement could be attributed to the presence of phenolic groups inherent in OEO. Another peak was observed between 3000 cm⁻¹ and 2750 cm⁻¹ and related to C–H stretching vibrations of –CH₂ (Arfat et al., 2014). The higher amplitudes of these peaks after the addition of OEO could be attributed to the symmetrical stretching of methylene hydrocarbons present in OEO incorporated into the film matrix (Arfat et al., 2014). In addition, characteristic peaks corresponding to amide I (1641 cm⁻¹), amide II (1535 cm⁻¹), and amide III (1260 cm⁻¹ and 1226 cm⁻¹) were observed in all PPI-based films. The intensity of these peaks gradually increased with the addition of OEO, and the 1260 cm⁻¹ peak exhibited a shift to 1226 cm⁻¹, indicating the presence of interaction between PPI and OEO molecules. The peak at 1406 cm⁻¹ may be correlated with symmetric stretching of the carboxylate group (Almasi et al., 2021), while the peak at 1041 cm⁻¹ was attributed to the existence of glycerol and its interaction with protein molecules (Yilmaz et al., 2020). Overall, the addition of OEO into the film matrix impacted on the interactions among OEO, protein, and glycerol molecules, as evidenced by the altered spectral profiles.

3.2.4. Moisture content (MC) and total soluble matter (TSM)

MC (moisture content) and TSM (total soluble matter) of the films are

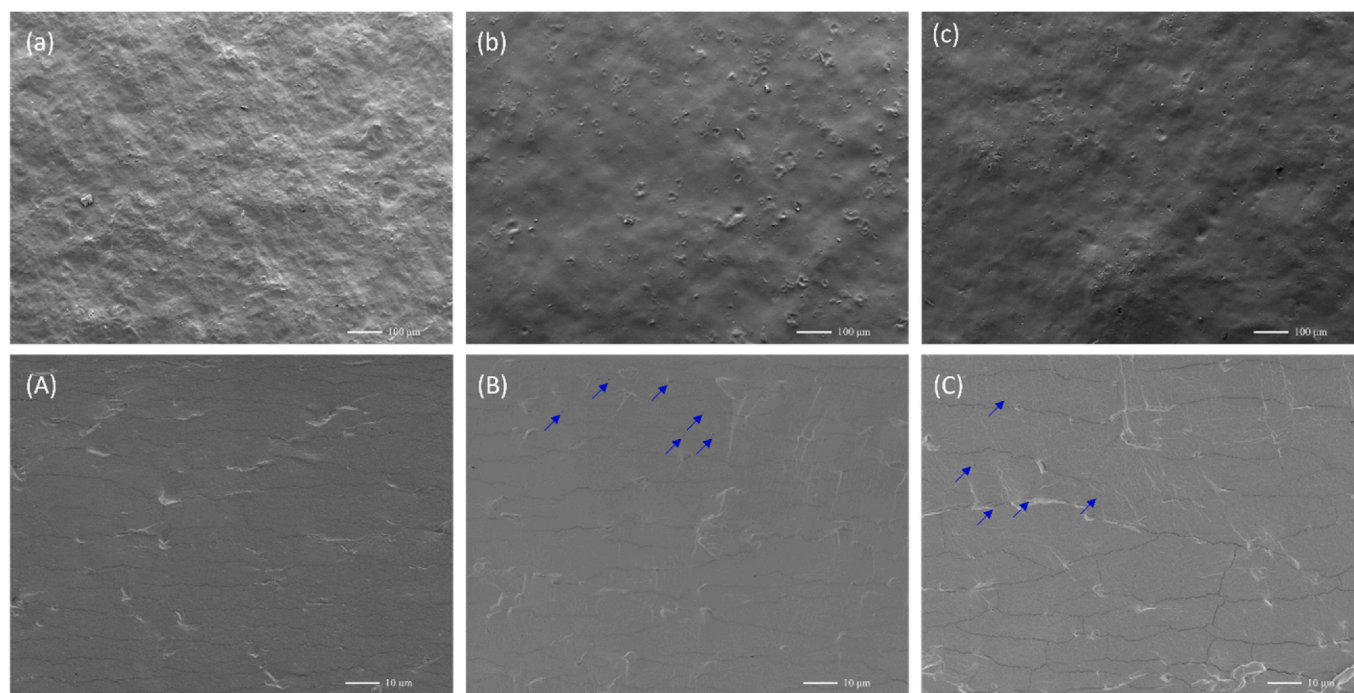


Fig. 2. The SEM images of the surface ($100\times$) (lowercase letters) and cross section ($1000\times$) (uppercase letters) of pea protein-based active films containing micro- (MOEO) or nano- (NOEO) oregano essential oil. a/A: PPI film; b/B: 2.0 % MOEO film; c/C: 2.0 % NOEO film.

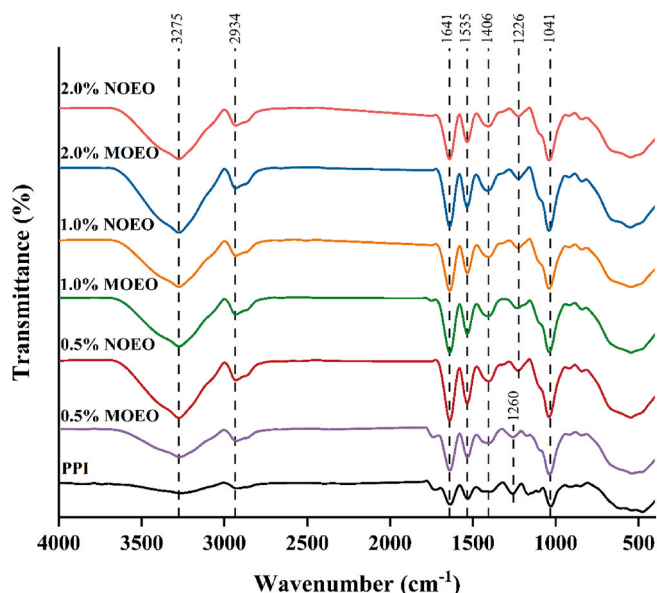


Fig. 3. The FTIR spectra of pea protein-based active films containing micro- (MOEO) or nano- (NOEO) oregano essential oil.

shown in [Table 1](#). For the pure PPI film, the MC and TSM were 26.50 % and 31.19 %, respectively. These results align with those of a previous study, which reported that the MC and TSM of PPI film fall within the range of 20.62–27.51 % and 24.95–29.75 %, respectively ([Gao et al., 2023](#)). Furthermore, it was found that the inclusion of OEO did not induce significant changes in the MC and TSM of the PPI film. A consistent finding was reported by [Zhang et al. \(2021\)](#) who incorporated thyme essential oil emulsion into gellan gum-chitosan film. However, some studies suggest that adding essential oils can lead to a decrease in the MC and TSM of the film, which may be attributed to the hydrophobic nature of essential oils ([Hasheminya and Dehghannya, 2021](#); [Yu et al.,](#)

[2022](#)). In fact, MC and TSM are primarily influenced by the hygroscopic properties of the film ([Rumondor and Taylor, 2010](#)). When the amount of essential oil added is insufficient to influence the hygroscopicity of the film matrix, the solubility and moisture content of the film may not undergo significant changes. This could be one of the possible reasons for the nonsignificant changes in MC and TSM in our study.

3.2.5. Water vapor permeability (WVP)

Packaging film is crucial for protecting food from the moisture in the environment, and water vapor permeability (WVP) is a key measure to evaluate the film's effectiveness as a water barrier at a given temperature ([Long et al., 2023](#)). The WVP values are presented in [Table 1](#). Compared to the PPI film, the addition of OEO to the film matrix at a concentration of 0.5 % resulted in a decrease in WVP. This reduction was observed in both MOEO and NOEO films. However, as the concentration of OEO increased, the WVP values of the films also increased, reaching their highest level at the 2.0 % OEO concentration. The addition of essential oils in edible films can have different effects on the WVP of the films. On one hand, essential oils can slow down the moisture penetration rate by increasing the tortuosity of the pathway ([Haghighatpanah et al., 2022](#)). On the other hand, essential oils can cause phase separation within the film matrix, resulting in the enlargement of pore sizes in the film, and thereby increasing the diffusion of gases or vapors ([Cai and Wang, 2021](#); [Zhang et al., 2021](#)). In our samples, the addition of 0.5 % OEO could have increased the tortuosity of water molecule permeation within the intact film structure; however, an increased amount of OEO led to higher extent of phase separation within the film that facilitated the passage of water molecules, resulting in higher WVP values. Moreover, we observed that when the concentration of OEO exceeded 1.0 %, the WVP of NOEO film was significantly lower than that of MOEO film, indicating superior water vapor barrier property. This result is not surprising due to the smaller and more uniform dispersion of oil droplets in NOEO, they lessened the above-mentioned, exacerbated effects of incorporating oil droplets on the passage of moisture.

3.2.6. Water contact angle (WCA)

Water contact angle (WCA) is used to assess the wettability or

hydrophobicity of a solid surface (Zhao and Jiang, 2018). A surface is considered hydrophilic if the WCA value is less than 90° and hydrophobic with WCA value being greater than 90°. Table 1 shows the WCA of various PPI-based films. The WCA of pure PPI film was 57.94°, indicating a hydrophilic surface due to pea protein's hydrophilic properties. The addition of OEO to the PPI film resulted in a reduction in WCA, and this decreasing trend persisted even when using nano-emulsion. This is because the addition of hydrophobic compounds altered the hydrophobic interactions among protein molecules in the film-forming dispersion in a way that projects polar molecules to distribute onto the surface of the film, and thus leading to an increase in surface hydrophilicity (Munhuweyi et al., 2017). It should be noted that, contrary to the above explanation, the hydrophobic nature of essential oil may be able to increase the surface hydrophobicity of the film, as reported in other studies (Hasheminya and Dehghannya, 2021; Li et al., 2020). Additionally, the addition of essential oil noticeably alters the roughness of the film's surface (supported by the SEM results), which also affects the surface's hydrophilic-hydrophobic characteristics (Bikerman, 1950). In our study, the reduction in film surface hydrophobicity that was observed in PPI-OEO system may be the cumulative result of the combined effects of those factors.

3.2.7. Mechanical properties

The influence of various additions of OEO, whether in the form of micro-emulsion or nano-emulsion, on the tensile strength (TS) and elongation at break (EAB) of PPI films is detailed in Table 2. The TS and EAB values for PPI film were 0.92 MPa and 75.64 %, respectively. The addition of different concentrations of OEO resulted in a slight decrease in TS, reaching a minimum of 0.63 MPa for the film added with 1.0 % MOEO. The addition of OEO significantly reduced the EAB values, and with an increase in oil concentration, the EAB values further decreased, reaching a minimum of 39.44 %. These findings are consistent with previous studies, which indicated that the addition of essential oils reduces the TS and EAB of the films (Ghadetaj et al., 2018; Sogut, 2020; Zhang et al., 2021). Ghadetaj et al. (2018) attributed the reduction to the hydrophobic nature of essential oils weakening the intermolecular interactions among the film's polymers, disrupting the film's structure, and subsequently decreasing its mechanical properties. Nevertheless, an exception was noticed in our samples: the EAB value of the 0.5 % NOEO film surpassed both the 0.5 % MOEO film and the PPI film although this difference disappeared as the concentration increased. This initial increase in EAB could be due to the plasticizing effect of OEO at lower concentration, likely enhanced by a reduction in droplet size (Otoni et al., 2014b). At higher OEO concentrations, the plasticizing effect couldn't counteract the structural disruption caused by OEO in the PPI film, resulting in reduced mechanical resistance.

3.2.8. Color

The color of packaging materials can significantly impact consumer preferences. In Table 3, the influence of OEO addition on the color of PPI films is presented. Color characteristics are represented by *L*, *a*, and *b* values. The incorporation of OEO led to a decrease in *L* value and an increase in *b* value of the PPI film, with this trend becoming more

Table 2

The tensile strength (TS) and elongation at break (EAB) of pea protein-based active films containing micro- (MOEO) or nano- (NOEO) oregano essential oil.

Film samples	Tensile strength (MPa)	Elongation at break (%)
PPI	0.92 ± 0.16 ^{bc}	75.64 ± 1.85 ^c
0.5 % MOEO	0.84 ± 0.10 ^{abc}	60.04 ± 1.70 ^b
0.5 % NOEO	1.05 ± 0.10 ^c	95.81 ± 11.16 ^d
1.0 % MOEO	0.63 ± 0.12 ^a	39.44 ± 5.02 ^a
1.0 % NOEO	0.67 ± 0.05 ^a	42.67 ± 2.49 ^a
2.0 % MOEO	0.70 ± 0.15 ^{ab}	42.00 ± 10.29 ^a
2.0 % NOEO	0.84 ± 0.20 ^{abc}	48.48 ± 5.55 ^a

Different letters within the same column are significantly different ($p < 0.05$).

Table 3

The color of pea protein-based active films containing micro- (MOEO) or nano- (NOEO) oregano essential oil.

Film samples	<i>L</i>	<i>a</i>	<i>b</i>
PPI	84.32 ± 0.72 ^{bc}	-0.42 ± 0.40 ^{ab}	17.96 ± 1.73 ^{ab}
0.5 % MOEO	83.91 ± 0.45 ^{bc}	-0.19 ± 0.26 ^{ab}	18.79 ± 0.24 ^{abc}
0.5 % NOEO	85.21 ± 0.58 ^c	-0.90 ± 0.13 ^a	16.42 ± 2.09 ^a
1.0 % MOEO	82.86 ± 0.73 ^{ab}	0.07 ± 0.52 ^{ab}	21.14 ± 0.75 ^{cd}
1.0 % NOEO	81.77 ± 0.92 ^a	0.59 ± 0.10 ^b	20.55 ± 0.75 ^{bcd}
2.0 % MOEO	82.38 ± 1.59 ^a	0.42 ± 1.34 ^b	23.24 ± 3.26 ^d
2.0 % NOEO	81.46 ± 1.23 ^a	0.29 ± 0.66 ^b	22.66 ± 1.46 ^d

Different letters within the same column are significantly different ($p < 0.05$).

pronounced as the concentration of OEO increased. Similar results have been reported by previous studies, who incorporated OEO into alginate films and quince seed mucilage films (Benavides et al., 2012; Jouki et al., 2014b). The obvious change in color is attributed to the inherent yellow color of OEO.

3.2.9. Antimicrobial activity

Salmonella is a prevalent pathogenic bacterium commonly present in chicken (Hai et al., 2020). To assess the antimicrobial properties of PPI-based films containing OEO and to determine potential differences in the antibacterial effects between MOEO and NOEO films, the in vitro antibacterial efficacy of the films was tested against three *Salmonella* strains by measuring inhibition zones. Only data from films containing 2.0 % MOEO and NOEO are shown in Table 4 since no inhibition zones were observed at OEO concentrations of 0.5 % and 1.0 %. Moreover, 2.0 % was identified as the preferable concentration, enabling the film to maintain both packaging properties and antibacterial activity. As shown, the PPI film without OEO did not exhibit any inhibition zones, whereas the 2.0 % MOEO and 2.0 % NOEO films demonstrated strong antibacterial activity against all three *Salmonella* strains, with inhibition zone diameters ranging from 23.00 to 27.80 mm. Additionally, there was no significant difference in the size of the inhibition zones between MOEO and NOEO films against the same strain of *Salmonella*. This indicated that the addition of OEO indeed imparts antibacterial properties to the PPI film. Furthermore, compared to the micro-scale droplets, OEO distributed at a smaller nano-scale level within the film did not significantly enhance its antibacterial efficacy against *Salmonella*. Instead, the concentration of OEO appeared to be the critical factor determining its antibacterial effects.

Many studies suggested that reducing the droplet size of essential oil significantly increased its antimicrobial effectiveness (Ghadetaj et al., 2018; Liu et al., 2022). This is because the reduction in droplet size increases the surface area available for essential oil to interact with bacterial cell membranes, leading to greater disruption of the membrane's permeability that ultimately results in cell apoptosis (Zhang et al., 2021). However, some other studies, similar to our findings here, reported the opposite. For example, Liao et al. (2021) and Buranasuksombat et al. (2011) found that the size of oil droplets did not significantly change the antibacterial properties of trans-cinnamaldehyde and lemon myrtle oil emulsions, respectively. They noted that reducing droplet size does not necessarily enhance the antibacterial effectiveness of essential oil emulsions. Our data also

Table 4

Antimicrobial activity of pea protein-based active films containing micro- (MOEO) or nano- (NOEO) oregano essential oil.

Film samples	Inhibition zone (mm)		
	<i>S. Typhimurium</i>	<i>S. Infantis</i>	<i>S. Enteritidis</i>
PPI	ND	ND	ND
2.0 % MOEO	27.80 ± 2.55 ^a	26.80 ± 1.41 ^a	27.00 ± 0.57 ^a
2.0 % NOEO	25.10 ± 0.42 ^a	24.80 ± 1.13 ^a	23.00 ± 2.26 ^a

Different letters within the same column are significantly different ($p < 0.05$).

supports this argument as the antimicrobial activity of essential oils depends on the overall interactions between oil and film matrix, and thus the effect of oil droplet size on the antimicrobial activity is on a case-by-case basis. This also highlights the importance of the current study in illustrating the antimicrobial activity of OEO when it is incorporated in pea protein film matrix. In addition, our results indicated that adding OEO to the PPI film matrix may not necessarily require the preparation of OEO nano-emulsions; satisfactory antimicrobial effects can be achieved with micron-sized emulsions.

3.3. Microbiological analysis of chicken breast

Chicken breast was utilized as a model food system to evaluate the antimicrobial activity of PPI-based films containing OEO. The aerobic plate count (APC) of chicken breast samples stored at 4 °C for 10 days was measured (Fig. 4). The fresh chicken breast had an APC load of approximately 2.00 Log CFU/g on the initial day. As the storage time extended, the APC values increased gradually in all groups, but the growth rates varied. Among them, the control group, which refers to chicken breast stored without any treatment, exhibited the fastest microbial growth. Compared to the control group, chicken breast packaged by plastic films did not slow down the microbial growth rate. In contrast, the chicken samples treated with PPI film without any OEO exhibited a significant inhibition of microbial growth in the first two days of storage, as evidenced by notably lower APC value. This effect may be attributed to the natural antimicrobial substances present in pea protein (Saad et al., 2017). However, as the storage time extended, by day 6, there were no significant differences in APC values among above mentioned 3 groups (control, plastic film, and PPI film groups), and all groups exceeded 7.80 Log CFU/g, surpassing the acceptable limit (7.00 Log CFU/g). When examining chicken samples coated and packaged by PPI-based active films, their APC values increased with storage time but remained significantly lower than those of the control, plastic film, and PPI film groups. Specifically, on day 4, the addition of 1.0 % COEO and 2.0 % COEO could significantly reduce the APC values of chicken breast by 17.89 % and 33.28 %, respectively, compared to the control. After day 4, the APC values of the treatment groups with OEO addition consistently remained lower than those of the treatment groups without OEO addition. These results indicated that incorporating OEO into PPI films indeed suppressed microbial growth in chicken breast. Similarly, Karimnezhad et al. (2019) reported a significant decrease in APC values of chicken breast with the addition of OEO to chitosan film. However, the antibacterial activity of OEO differs in these two studies. In their research, the addition of 1.0 % OEO to chitosan film reduced the APC value to 4.23 Log CFU/g on day 6. In contrast, our results showed that the APC value of 1.0 % OEO treated sample on day 6 was reduced to 6.67–6.99 Log CFU/g. The discrepancy indicates that the antibacterial effects of essential oils vary in different film matrices. Furthermore, the antimicrobial effect significantly improved with an increase in the addition of OEO. However, at the same level of OEO content, there was no significant difference in APC values between the MOEO and NOEO film treatments. This showed that the particle size of OEO in the film did not have a significant impact on the inhibitory effect on surface bacteria of chicken breast, which also validated the previous results on the in vitro antimicrobial activity (Section 3.2.9). It was interesting to observe that after the 8-day storage, there was no significant change in APC values for all samples. This may be due to the inhibitory metabolites of microbial growth in the stationary stage, making the environment less conducive for further microbial growth (Maier and Pepper, 2015). Similar results have been observed by other studies (Javaherzadeh et al., 2020; Nouri Ala and Shahbazi, 2019; Zheng et al., 2023).

4. Conclusion

To summary, we successfully incorporated OEO into the PPI film matrix and fabricated PPI-based active films with antimicrobial

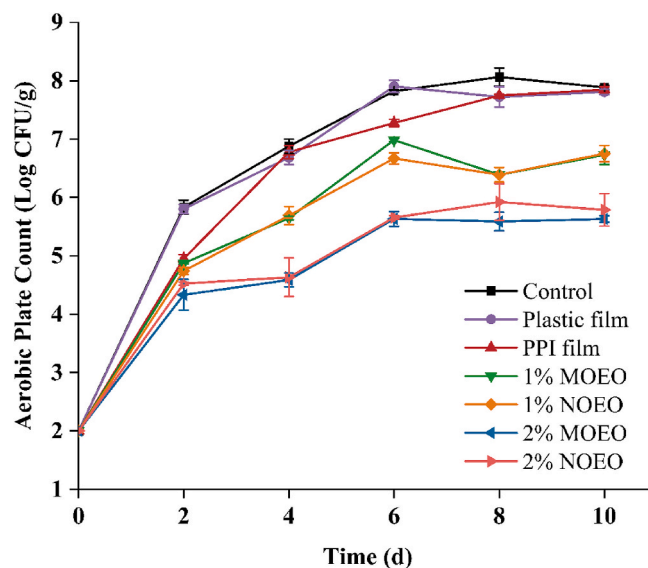


Fig. 4. The aerobic plate count (APC) of chicken breast samples treated without packaging, with plastic film packaging, or with PPI films containing different amounts of micro- (MOEO) or nano- (NOEO) oregano essential oil during 10 days of refrigerated storage (4 °C).

properties. Changes in film structure and variations in chemical bond strength, as determined by SEM and FTIR, confirmed the presence of OEO within the PPI film. The addition of OEO significantly altered film properties, including mechanical properties, water resistance, color, and thickness. These alterations were primarily associated with the concentration of added OEO rather than its particle size. PPI-based film with 2.0 % OEO exhibited a notable antibacterial effect, showing significant inhibition of the growth of three *Salmonella* strains. Application of PPI-based film with 2.0 % OEO on chicken breast also revealed significant inhibition of the bacteria, delaying the spoilage for 5 days. Furthermore, reducing the particle size of OEO to the nano-scale did not significantly enhance its antimicrobial effectiveness in the PPI film. Taken together, the addition of OEO into PPI-based film proved to be an efficient method for enhancing its antimicrobial activity. The resultant antibacterial film demonstrated substantial potential for application on chicken breast.

Funding

This work was supported by the Council on Research & Creativity, Florida State University (135000-551-046339, 2022).

CRedit authorship contribution statement

Jingjing Cheng: Investigation, Formal analysis, Writing – original draft, preparation. **Frank J. Velez:** Investigation, Formal analysis. **Prashant Singh:** Conceptualization, Formal analysis, Writing – review & editing. **Leqi Cui:** Conceptualization, Supervision, Writing – review & editing.

Declaration of competing interest

There are no conflicts to declare.

Data availability

Data will be made available on request.

References

- Almasi, L., Radi, M., Amiri, S., McClements, D.J., 2021. Fabrication and characterization of antimicrobial biopolymer films containing essential oil-loaded microemulsions or nanoemulsions. *Food Hydrocolloids* 117, 106733. <https://doi.org/10.1016/j.foodhyd.2021.106733>.
- Arfat, Y.A., Benjakul, S., Prodpran, T., Sumpavapol, P., Songtipya, P., 2014. Properties and antimicrobial activity of fish protein isolate/fish skin gelatin film containing basil leaf essential oil and zinc oxide nanoparticles. *Food Hydrocolloids* 41, 265–273. <https://doi.org/10.1016/j.foodhyd.2014.04.023>.
- ASTM, 1995. *Standard Test Methods for Water Vapor Transmission of Materials 1*.
- Atarés, L., Chiralt, A., 2016. Essential oils as additives in biodegradable films and coatings for active food packaging. *Trends Food Sci. Technol.* 48, 51–62. <https://doi.org/10.1016/j.tifs.2015.12.001>.
- Avila-Sosa, R., Palou, E., Jiménez Munguía, M.T., Nevárez-Moorillón, G.V., Navarro Cruz, A.R., López-Malo, A., 2012. Antifungal activity by vapor contact of essential oils added to amaranth, chitosan, or starch edible films. *Int. J. Food Microbiol.* 153, 66–72. <https://doi.org/10.1016/j.ijfoodmicro.2011.10.017>.
- Benavides, S., Villalobos-Carvajal, R., Reyes, J.E., 2012. Physical, mechanical and antibacterial properties of alginate film: effect of the crosslinking degree and oregano essential oil concentration. *J. Food Eng.* 110, 232–239. <https://doi.org/10.1016/j.jfoodeng.2011.05.023>.
- Bhavanirama, S., Vishnupriya, S., Al-Aboudy, M.S., Vijayakumar, R., Baskaran, D., 2019. Role of essential oils in food safety: antimicrobial and antioxidant applications. *Grain Oil Sci. Technol.* 2, 49–55. <https://doi.org/10.1016/j.gaost.2019.03.001>.
- Bikerman, J.J., 1950. Surface roughness and contact angle. *J. Phys. Colloid Chem.* 54, 653–658.
- Bonfanti, C., Ianni, R., Mazzaglia, A., Lanza, C.M., Napoli, E.M., Ruberto, G., 2012. Emerging cultivation of oregano in Sicily: sensory evaluation of plants and chemical composition of essential oils. *Ind. Crops Prod.* 35, 160–165. <https://doi.org/10.1016/j.indcrop.2011.06.029>.
- Buranasukombat, U., Kwon, Y.J., Turner, M., Bhandari, B., 2011. Influence of emulsion droplet size on antimicrobial properties. *Food Sci. Biotechnol.* 20, 793–800. <https://doi.org/10.1007/s10068-011-0110-x>.
- Cai, L., Wang, Y., 2021. Physicochemical and antioxidant properties based on fish sarcoplasmic protein/chitosan composite films containing ginger essential oil nanoemulsion. *Food Bioprocess Technol.* 14, 151–163. <https://doi.org/10.1007/s11947-020-02564-0>.
- Cai, L., Wang, Y., Cao, A., 2020. The physicochemical and preservation properties of fish sarcoplasmic protein/chitosan composite films containing ginger essential oil emulsions. *J. Food Process. Eng.* 43, 1–12. <https://doi.org/10.1111/jfpe.13495>.
- Chen, H., Wang, J., Cheng, Y., Wang, C., Liu, H., Bian, H., Pan, Y., Sun, J., Han, W., 2019. Application of protein-based films and coatings for food packaging: a review. *Polymers (Basel)* 11. <https://doi.org/10.3390/polym11122039>.
- Cheng, J., Cui, L., 2021. Effects of high-intensity ultrasound on the structural, optical, mechanical and physicochemical properties of pea protein isolate-based edible film. *Ultrason. Sonochem.* 80, 105809. <https://doi.org/10.1016/j.ultrsonch.2021.105809>.
- Cheng, J., Li, Z., Wang, J., Zhu, Z., Yi, J., Chen, B., Cui, L., 2022. Structural characteristics of pea protein isolate (PPI) modified by high-pressure homogenization and its relation to the packaging properties of PPI edible film. *Food Chem.* 388, 132974. <https://doi.org/10.1016/j.foodchem.2022.132974>.
- Cheng, J., Wang, J., Cui, L., 2023. Incorporation of α -tocopherol into pea protein edible film using pH-shifting and nanoemulsion treatments: enhancing its antioxidant activity without negative impacts on mechanical properties. *Foods* 12. <https://doi.org/10.3390/foods12102022>.
- Choi, W.S., Han, J.H., 2001. Physical and mechanical properties of pea-protein-based edible films. *J. Food Sci.* 66, 319–322. <https://doi.org/10.1111/j.1365-2621.2001.tb11339.x>.
- Cui, L., Shen, P., Gao, Z., Yi, J., Chen, B., 2019. New insights into the impact of sodium chloride on the lipid oxidation of oil-in-water emulsions. *J. Agric. Food Chem.* 67, 4321–4327. <https://doi.org/10.1021/acs.jafc.9b00396>.
- Donsi, F., Ferrari, G., 2016. Essential oil nanoemulsions as antimicrobial agents in food. *J. Biotechnol.* 233, 106–120. <https://doi.org/10.1016/j.jbiotec.2016.07.005>.
- Gao, X., Dai, Y., Cao, J., Hou, H., 2023. Analysis of the effect mechanism of wet grinding on the film properties of pea protein isolate based on its structure changes. *Innovat. Food Sci. Emerg. Technol.* 89, 103474. <https://doi.org/10.1016/j.ifset.2023.103474>.
- Ge, J., Sun, C.X., Corke, H., Gul, K., Gan, R.Y., Fang, Y., 2020. The health benefits, functional properties, modifications, and applications of pea (*Pisum sativum* L.) protein: current status, challenges, and perspectives. *Compr. Rev. Food Sci. Food Saf.* 19, 1835–1876. <https://doi.org/10.1111/1541-4337.12573>.
- Ghadetaj, A., Almasi, H., Mehryar, L., 2018. Development and characterization of whey protein isolate active films containing nanoemulsions of Grammosciadium pterocarpum Bioss. essential oil. *Food Packag. Shelf Life* 16, 31–40. <https://doi.org/10.1016/j.fpsl.2018.01.012>.
- Ghamari, M.A., Amiri, S., Rezaazadeh-Bari, M., Rezaazadeh-Bari, L., 2022. Physical, mechanical, and antimicrobial properties of active edible film based on milk proteins incorporated with *Nigella sativa* essential oil. *Polym. Bull.* 79, 1097–1117. <https://doi.org/10.1007/s00289-021-03550-y>.
- Haghighatpanah, N., Omar-Aziz, M., Gharaghani, M., Khodaiyan, F., Hosseini, S.S., Kennedy, J.F., 2022. Effect of mung bean protein isolate/pullulan films containing marjoram (*Origanum majorana* L.) essential oil on chemical and microbial properties of minced beef meat. *Int. J. Biol. Macromol.* 201, 318–329. <https://doi.org/10.1016/j.jbiomac.2022.01.023>.
- Hai, D., Yin, X., Lu, Z., Lv, F., Zhao, H., Bie, X., 2020. Occurrence, drug resistance, and virulence genes of *Salmonella* isolated from chicken and eggs. *Food Control* 113, 107109. <https://doi.org/10.1016/j.foodcont.2020.107109>.
- Hao, Y., Kang, J., Yang, R., Li, H., Cui, H., Bai, H., Tsitsilin, A., Li, J., Shi, L., 2022. Multidimensional exploration of essential oils generated via eight oregano cultivars: compositions, chemodiversities, and antibacterial capacities. *Food Chem.* 374, 131629. <https://doi.org/10.1016/j.foodchem.2021.131629>.
- Hasheminya, S.M., Dehghannya, J., 2021. Development and characterization of novel edible films based on Cordia dichotoma gum incorporated with *Salvia mirzayanii* essential oil nanoemulsion. *Carbohydr. Polym.* 257, 117606. <https://doi.org/10.1016/j.carbpol.2020.117606>.
- Hashim, S.B.H., Tahir, H.E., Mahdi, A.A., Zhang, J., Zhai, X., Al-Maqtari, Q.A., Zhou, C., Mahunu, G.K., Xiaobo, Z., Jiyong, S., 2024. Enhancement of a hybrid colorimetric film incorporating *Origanum compactum* essential oil as antibacterial and monitor chicken breast and shrimp freshness. *Food Chem.* 432, 137203. <https://doi.org/10.1016/j.foodchem.2023.137203>.
- Hematizad, I., Khanjari, A., Basti, A.A., Karabagias, I.K., Noori, N., Ghadami, F., Gholami, F., Teimourifard, R., 2021. In vitro antibacterial activity of gelatin-nanochitosan films incorporated with *Zataria multiflora* Boiss essential oil and its influence on microbial, chemical, and sensorial properties of chicken breast meat during refrigerated storage. *Food Packag. Shelf Life* 30, 100751. <https://doi.org/10.1016/j.fpsl.2021.100751>.
- Hudzicki, J., 2009. Kirby-Bauer disk diffusion susceptibility test protocol author information. *Am. Soc. Microbiol.* 1–23.
- Javaheerzadeh, R., Tabatabaee Bafroee, A.S., Kanjari, A., 2020. Preservation effect of Polylophium involucreatum essential oil incorporated poly lactic acid/nanochitosan composite film on shelf life and sensory properties of chicken fillets at refrigeration temperature. *Lwt* 118, 108783. <https://doi.org/10.1016/j.lwt.2019.108783>.
- Jouki, M., Mortazavi, S.A., Yazdi, F.T., Koocheki, A., Khazaei, N., 2014a. Use of quince seed mucilage edible films containing natural preservatives to enhance physico-chemical quality of rainbow trout fillets during cold storage. *Food Sci. Hum. Wellness* 3, 65–72. <https://doi.org/10.1016/j.fshw.2014.05.002>.
- Jouki, M., Yazdi, F.T., Mortazavi, S.A., Koocheki, A., 2014b. Quince seed mucilage films incorporated with oregano essential oil: physical, thermal, barrier, antioxidant and antibacterial properties. *Food Hydrocolloids* 36, 9–19. <https://doi.org/10.1016/j.foodhyd.2013.08.030>.
- Karimnezhad, F., Razavilar, V., Anvar, A.A., Dashtgol, S., Zavareh, A.P., 2019. Combined effect of chitosan-based edible film containing oregano essential oil on the shelf-life extension of fresh chicken meat. *J. Nutr. Food Secur.* 4, 236–242. <https://doi.org/10.18502/JNFS.V4I4.1720>.
- Lam, A.C.Y., Can Karaca, A., Tyler, R.T., Nickerson, M.T., 2018. Pea protein isolates: structure, extraction, and functionality. *Food Rev. Int.* <https://doi.org/10.1080/87559129.2016.1242135>.
- Li, X., Yang, X., Deng, H., Guo, Y., Xue, J., 2020. Gelatin films incorporated with thymol nanoemulsions: physical properties and antimicrobial activities. *Int. J. Biol. Macromol.* 150, 161–168. <https://doi.org/10.1016/j.jbiomac.2020.02.066>.
- Liao, W., Dumas, E., Ghnimi, S., Elaissari, A., Gharsallaoui, A., 2021. Effect of emulsifier and droplet size on the antibacterial properties of emulsions and emulsion-based films containing essential oil compounds. *J. Food Process. Preserv.* 45, 1–10. <https://doi.org/10.1111/jfpp.16072>.
- Liu, M., Pan, Y., Feng, M., Guo, W., Fan, X., Feng, L., Huang, J., Cao, Y., 2022. Garlic essential oil in water nanoemulsion prepared by high-power ultrasound: properties, stability and its antibacterial mechanism against MRSA isolated from pork. *Ultrason. Sonochem.* 90, 106201. <https://doi.org/10.1016/j.ultrsonch.2022.106201>.
- Llana-Ruiz-Cabello, M., Pichardo, S., Bermúdez, J.M., Baños, A., Núñez, C., Guillamón, E., Aucejo, S., Cameán, A.M., 2016. Development of PLA films containing oregano essential oil (*Origanum vulgare* L. virens) intended for use in food packaging. *Food Addit. Contam. Part A Chem. Anal. Control. Expo. Risk Assess.* 33, 1374–1386. <https://doi.org/10.1080/19440049.2016.1204666>.
- Long, J., Zhang, W., Zhao, M., Ruan, C.Q., 2023. The reduce of water vapor permeability of polysaccharide-based films in food packaging: a comprehensive review. *Carbohydr. Polym.* 321, 121267. <https://doi.org/10.1016/j.carbpol.2023.121267>.
- Lu, Z.X., He, J.F., Zhang, Y.C., Bing, D.J., 2020. Composition, physicochemical properties of pea protein and its application in functional foods. *Crit. Rev. Food Sci. Nutr.* <https://doi.org/10.1080/10408398.2019.1651248>.
- Maier, R.M., Pepper, I.L., 2015. Bacterial growth. *Environ. Microbiol.* 37–54. <https://doi.org/10.1016/B978-0-12-370519-8.00003-1>. Third Ed.
- Munhuweyi, K., Caleb, O.J., Lennox, C.L., van Reenen, A.J., Opara, U.L., 2017. In vitro and in vivo antifungal activity of chitosan-essential oils against pomegranate fruit pathogens. *Postharvest Biol. Technol.* 129, 9–22. <https://doi.org/10.1016/j.postharvbio.2017.03.002>.
- Muñoz, L.A., Aguilera, J.M., Rodríguez-Turiénzo, L., Cobos, A., Diaz, O., 2012. Characterization and microstructure of films made from mucilage of *Salvia hispanica* and whey protein concentrate. *J. Food Eng.* 111, 511–518. <https://doi.org/10.1016/j.jfoodeng.2012.02.031>.
- Nor Bainun, I., Alias, N.H., Syed-Hassan, S.S.A., 2015. Nanoemulsion: formation, characterization, properties and applications - a review. *Adv. Mater. Res.* 1113, 147–152. <https://doi.org/10.4028/www.scientific.net/amr.1113.147>.
- Nouri Ala, M.A., Shahbazi, Y., 2019. The effects of novel bioactive carboxymethyl cellulose coatings on food-borne pathogenic bacteria and shelf life extension of fresh and sauced chicken breast fillets. *Lwt* 111, 602–611. <https://doi.org/10.1016/j.lwt.2019.05.092>.
- Otoni, C.G., Moura, M.R.d., Aouada, F.A., Camilloto, G.P., Cruz, R.S., Lorevice, M.V., Soares, N. de F.F., Mattoso, L.H.C., 2014a. Antimicrobial and physical-mechanical properties of pectin/papaya puree/cinnamaldehyde nanoemulsion edible composite

- films. *Food Hydrocolloids* 41, 188–194. <https://doi.org/10.1016/j.foodhyd.2014.04.013>.
- Otoni, C.G., Pontes, S.F.O., Medeiros, E.A.A., Soares, N.D.F.F., 2014b. Edible films from methylcellulose and nanoemulsions of clove bud (*Syzygium aromaticum*) and oregano (*Origanum vulgare*) essential oils as shelf life extenders for sliced bread. *J. Agric. Food Chem.* 62, 5214–5219. <https://doi.org/10.1021/jf501055f>.
- Rumondor, A.C.F., Taylor, L.S., 2010. Effect of polymer hygroscopicity on the phase behavior of amorphous solid dispersions in the presence of moisture. *Mol. Pharm.* 7, 477–490. <https://doi.org/10.1021/mp9002283>.
- Saad, A.M., Elmassry, R.A., Wahdan, K.M., Osman, A.O., 2017. Chemical characterization, antimicrobial and antioxidant activity of 7S and 11S globulins isolated from pea (*Pisum sativum*). *Zagazig J. Agric. Res.* 44, 2221–2230. <https://doi.org/10.21608/zjar.2017.51290>.
- Salvia-Trujillo, L., Rojas-Gräu, A., Soliva-Fortuny, R., Martín-Belloso, O., 2015. Physicochemical characterization and antimicrobial activity of food-grade emulsions and nanoemulsions incorporating essential oils. *Food Hydrocolloids* 43, 547–556. <https://doi.org/10.1016/j.foodhyd.2014.07.012>.
- Sogut, E., 2020. Active whey protein isolate films including bergamot oil emulsion stabilized by nanocellulose. *Food Packag. Shelf Life* 23, 100430. <https://doi.org/10.1016/j.foodpsl.2019.100430>.
- Teixeira, B., Marques, A., Pires, C., Ramos, C., Batista, I., Saraiva, J.A., Nunes, M.L., 2014. Characterization of fish protein films incorporated with essential oils of clove, garlic and oregano: physical, antioxidant and antibacterial properties. *Lwt* 59, 533–539. <https://doi.org/10.1016/j.lwt.2014.04.024>.
- Yang, X., Zhao, D., Ge, S., Bian, P., Xue, H., Lang, Y., 2023. Alginate-based edible coating with oregano essential oil/ β -cyclodextrin inclusion complex for chicken breast preservation. *Int. J. Biol. Macromol.* 251, 126126. <https://doi.org/10.1016/j.ijbiomac.2023.126126>.
- Yildirim, S., Röcker, B., Pettersen, M.K., Nilsen-Nygaard, J., Ayhan, Z., Rutkaite, R., Radusin, T., Suminska, P., Marcos, B., Coma, V., 2018. Active packaging applications for food. *Compr. Rev. Food Sci. Food Saf.* 17, 165–199. <https://doi.org/10.1111/1541-4337.12322>.
- Yilmaz, K., Turhan, S., Saricaoglu, F.T., Tural, S., 2020. Improvement of physicochemical, mechanical, thermal and surface properties of anchovy by-product protein films by addition of transglutaminase, and the correlation between secondary structure and mechanical properties. *Food Packag. Shelf Life* 24, 100483. <https://doi.org/10.1016/j.foodpsl.2020.100483>.
- Yıldırım-Yalçın, M., Sadıkoğlu, H., Şeker, M., 2021. Characterization of edible film based on grape juice and cross-linked maize starch and its effects on the storage quality of chicken breast fillets. *Lwt* 142. <https://doi.org/10.1016/j.lwt.2021.111012>.
- Yu, H., Zhang, C., Xie, Y., Mei, J., Xie, J., 2022. Effect of *Melissa officinalis* L. essential oil nanoemulsions on structure and properties of carboxymethyl chitosan/locust bean gum composite films. *Membranes (Basel)* 12. <https://doi.org/10.3390/membranes12060568>.
- Zhang, W., Jiang, H., Rhim, J.W., Cao, J., Jiang, W., 2022. Effective strategies of sustained release and retention enhancement of essential oils in active food packaging films/coatings. *Food Chem.* 367, 130671. <https://doi.org/10.1016/j.foodchem.2021.130671>.
- Zhang, X., Liu, D., Jin, T.Z., Chen, W., He, Q., Zou, Z., Zhao, H., Ye, X., Guo, M., 2021. Preparation and characterization of gellan gum-chitosan polyelectrolyte complex films with the incorporation of thyme essential oil nanoemulsion. *Food Hydrocolloids* 114. <https://doi.org/10.1016/j.foodhyd.2020.106570>.
- Zhao, R., Guan, W., Zhou, X., Lao, M., Cai, L., 2022. The physicochemical and preservation properties of anthocyanidin/chitosan nanocomposite-based edible films containing cinnamon-perilla essential oil pickering nanoemulsions. *Lwt* 153, 112506. <https://doi.org/10.1016/j.lwt.2021.112506>.
- Zhao, T., Jiang, L., 2018. Contact angle measurement of natural materials. *Colloids Surf. B Biointerfaces* 161, 324–330. <https://doi.org/10.1016/j.colsurfb.2017.10.056>.
- Zheng, K., Li, B., Liu, Y., Wu, D., Bai, Y., Xiang, Q., 2023. Effect of chitosan coating incorporated with oregano essential oil on microbial inactivation and quality properties of refrigerated chicken breasts. *Lwt* 176, 1–10. <https://doi.org/10.1016/j.lwt.2023.114547>.
- Zinoviadou, K.G., Koutsoumanis, K.P., Biliaderis, C.G., 2009. Physico-chemical properties of whey protein isolate films containing oregano oil and their antimicrobial action against spoilage flora of fresh beef. *Meat Sci.* 82, 338–345. <https://doi.org/10.1016/j.meatsci.2009.02.004>.